



# Automatic Detection of Nuclear Spins at Arbitrary Magnetic Fields via Signal-to-Image AI Model [1]

B. Varona-Uriarte<sup>1,2,\*</sup> C. Munuera-Javaloy<sup>1,2</sup> E. Terradillos<sup>3</sup> Y. Ban<sup>4,3</sup>  
A. Alvarez-Gila<sup>3</sup> E. Garrote<sup>3,5</sup> and J. Casanova<sup>1,2</sup>

<sup>1</sup>*Department of Physical Chemistry, University of the Basque Country UPV/EHU, Apartado 644, 48080 Bilbao, Spain*

<sup>2</sup>*EHU Quantum Center, University of the Basque Country UPV/EHU, Leioa, Spain*

<sup>3</sup>*TECNALIA, Basque Research and Technology Alliance (BRTA), Bizkaia Science and Technology Park, Astondo Bidea, Edificio 700, 48160 Derio, Spain*

<sup>4</sup>*Departamento de Física, Universidad Carlos III de Madrid, Avda. de la Universidad 30, 28911 Leganés, Spain*

<sup>5</sup>*Department of Automatic Control and Systems Engineering, University of the Basque Country UPV/EHU, 48013 Bilbao, Spain*



(Received 18 December 2023; accepted 11 March 2024; published 8 April 2024)

Quantum sensors leverage matter's quantum properties to enable measurements with unprecedented spatial and spectral resolution. Among these sensors, those utilizing nitrogen-vacancy (NV) centers in diamond offer the distinct advantage of operating at room temperature. Nevertheless, signals received from NV centers are often complex, making interpretation challenging. This is especially relevant in low magnetic field scenarios, where standard approximations for modeling the system fail. Additionally, NV signals feature a prominent noise component. In this Letter, we present a signal-to-image deep learning model capable of automatically inferring the number of nuclear spins surrounding a NV sensor and the hyperfine couplings between the sensor and the nuclear spins. Our model is trained to operate effectively across various magnetic field scenarios, requires no prior knowledge of the involved nuclei, and is designed to handle noisy signals, leading to fast characterization of nuclear environments in real experimental conditions. With detailed numerical simulations, we test the performance of our model in scenarios involving varying numbers of nuclei, achieving an average error of less than 2 kHz in the estimated hyperfine constants.

Borja Varona Uriarte  
14/10/2024

[1] B. Varona-Uriarte, C. Munuera-Javaloy, E. Terradillos, Y. Ban, A. Alvarez-Gila, E. Garrote, and J. Casanova, Phys. Rev. Lett. **132**, 150801 (2024).

# Outline

- **Motivation**
- **The system**
- **The SALI model**
  - 1D → 2D Convolutional Neural Network (CNN)
  - Image post-processing
- **Quantifying the model performance and results**
- **Reducing experimental time: high magnetic field**
- **Outlook and conclusions**

# Motivation

- Main objective: detect the coupling constants between the NV sensor and the surrounding  $^{13}\text{C}$  nuclear spins to characterize the system.

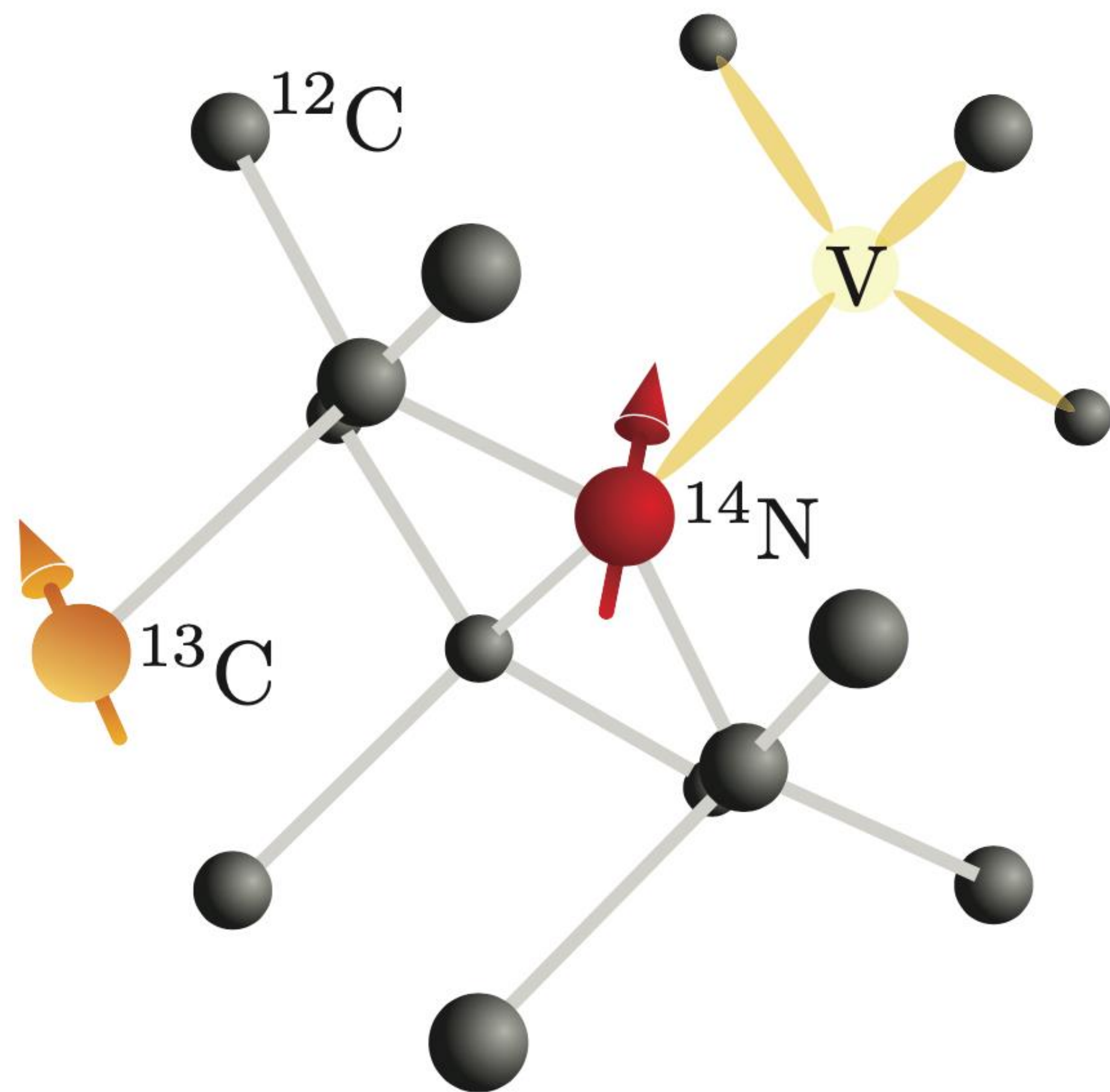
# Motivation

- Main objective: detect the coupling constants between the NV sensor and the surrounding  $^{13}\text{C}$  nuclear spins to characterize the system.
- Why a deep learning model?

# Motivation

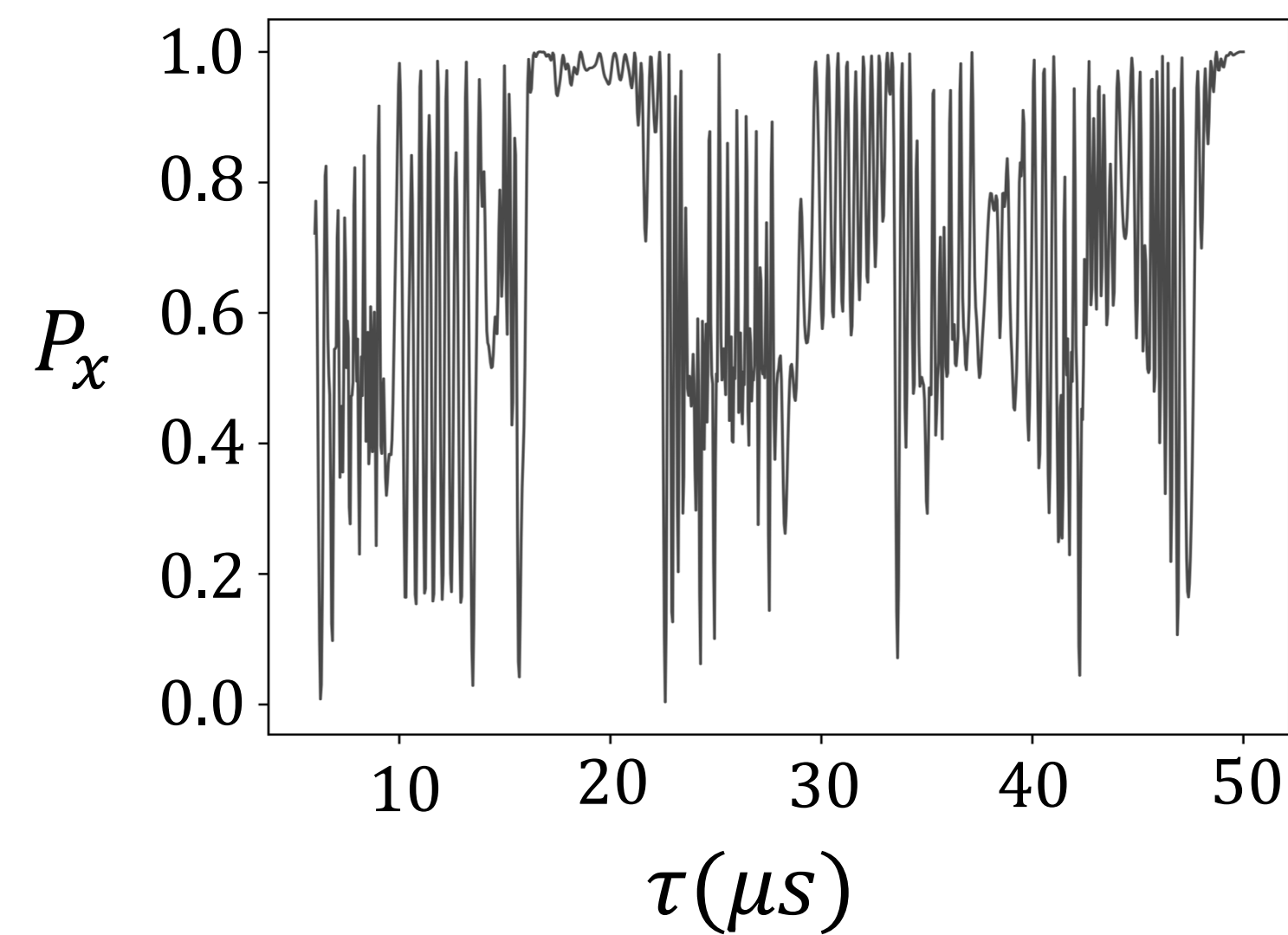
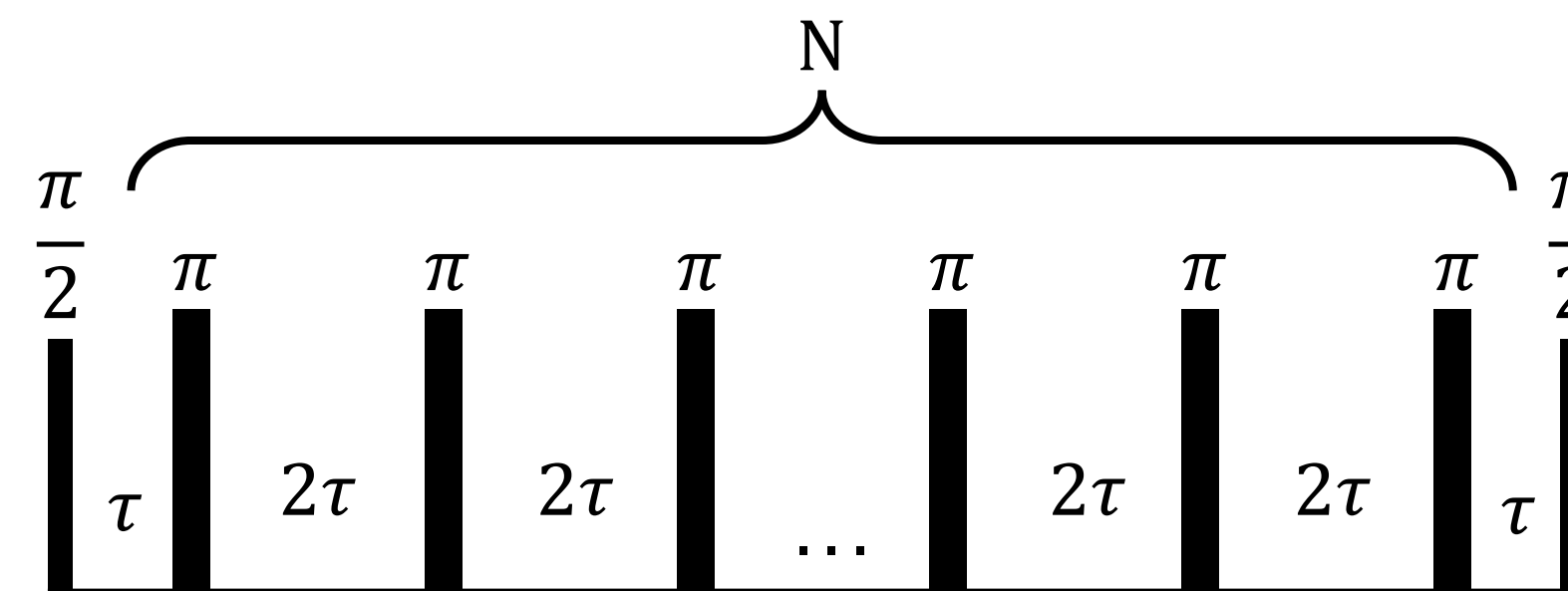
- Main objective: detect the coupling constants between the NV sensor and the surrounding  $^{13}\text{C}$  nuclear spins to characterize the system.
- Why a deep learning model?
  - Trained deep learning models offer fast characterization.
  - They are known to be robust to small perturbations in the input signals  $\longrightarrow$  great for real experimental conditions.
  - Our model, in particular, does not rely on specific characteristics of the input signal (resonance peaks, etc.)  $\longrightarrow$  applicable to both high and low magnetic field conditions.
  - It does not need previous knowledge of the number of nuclei present in the sample.

# The system



$$H_I = \sum_j \omega_j \hat{\omega}_j \cdot \vec{I}_j + \frac{f(t)}{2} \sigma_z \sum_j \vec{A}_j \cdot \vec{I}_j$$

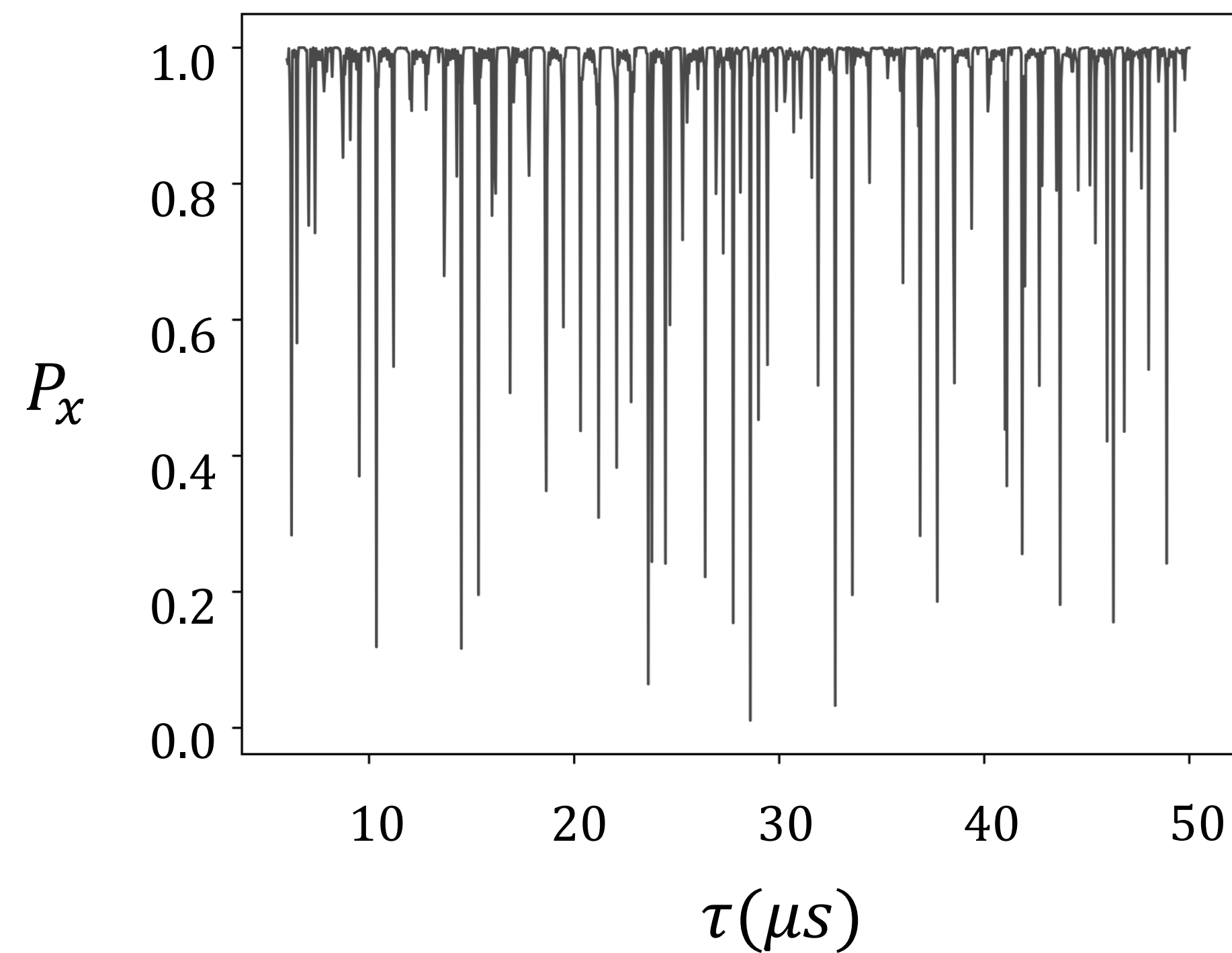
$$\vec{A}_j = (A_j^z, A_j^\perp)$$



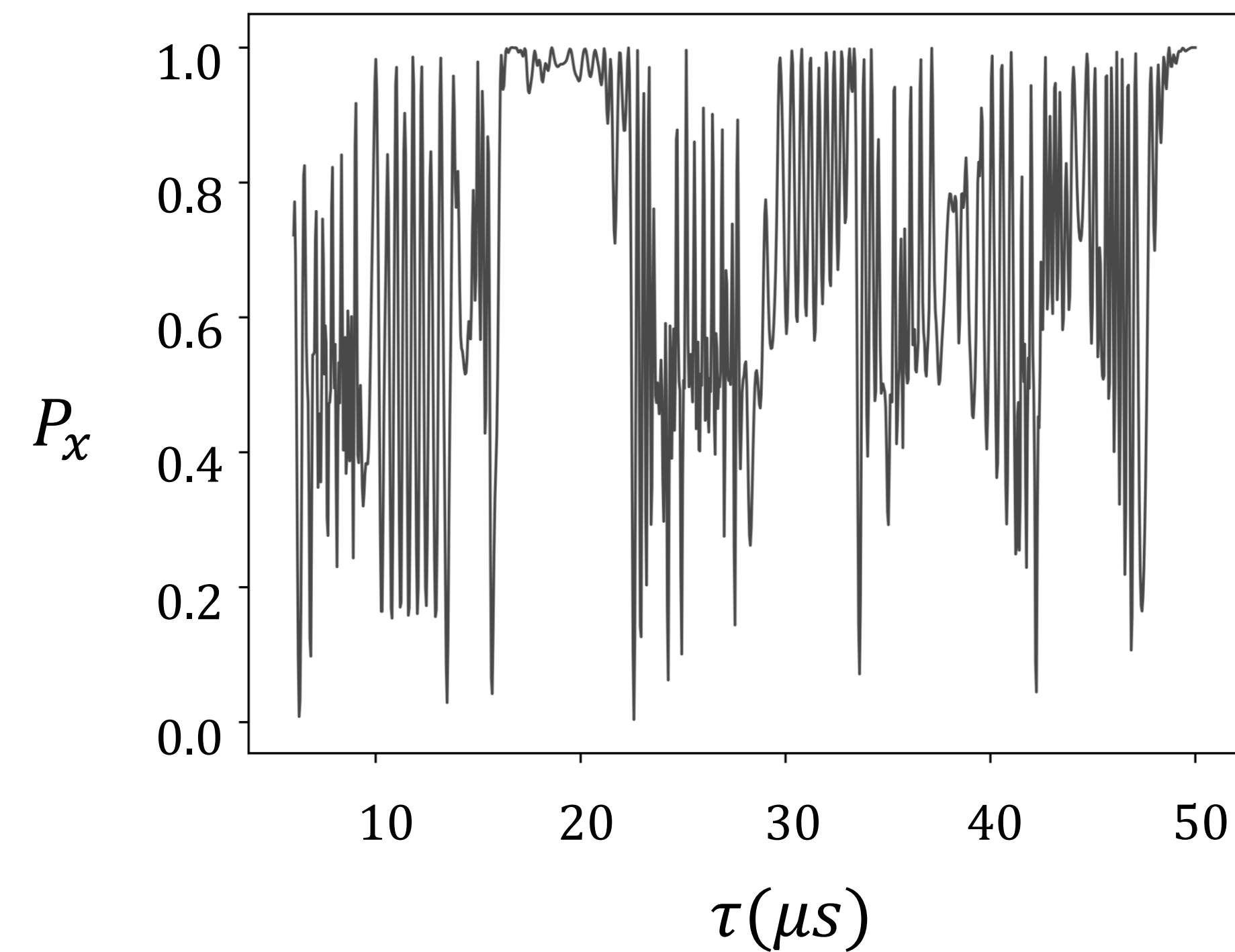
# The system

- $P_x$  calculated at  $B_z = 0.056$  T and  $B_z = 0.0056$  T.
- Each sequence contains  $N = 32$  pulses, and  $P_x$  is sampled  $N_p = 1000$  times in the range  $\tau \in [6, 50] \mu s$ .

**High field**



**Low field**



# The system

- Simulating real experimental conditions:

1. Decoherence

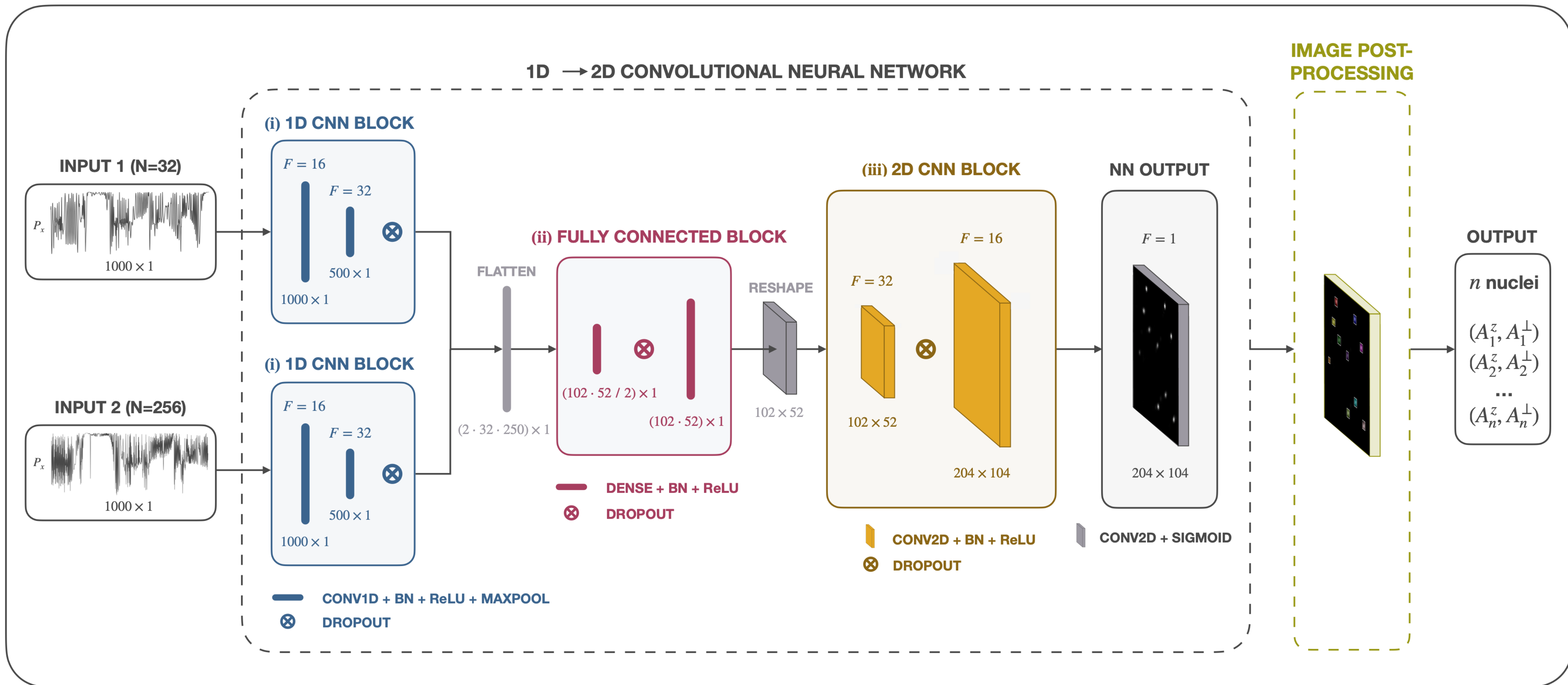
↳ multiplying by factor  $e^{-\tau/T_2}$  with  $T_2 = 200 \mu s$ .

2. Shot-noise

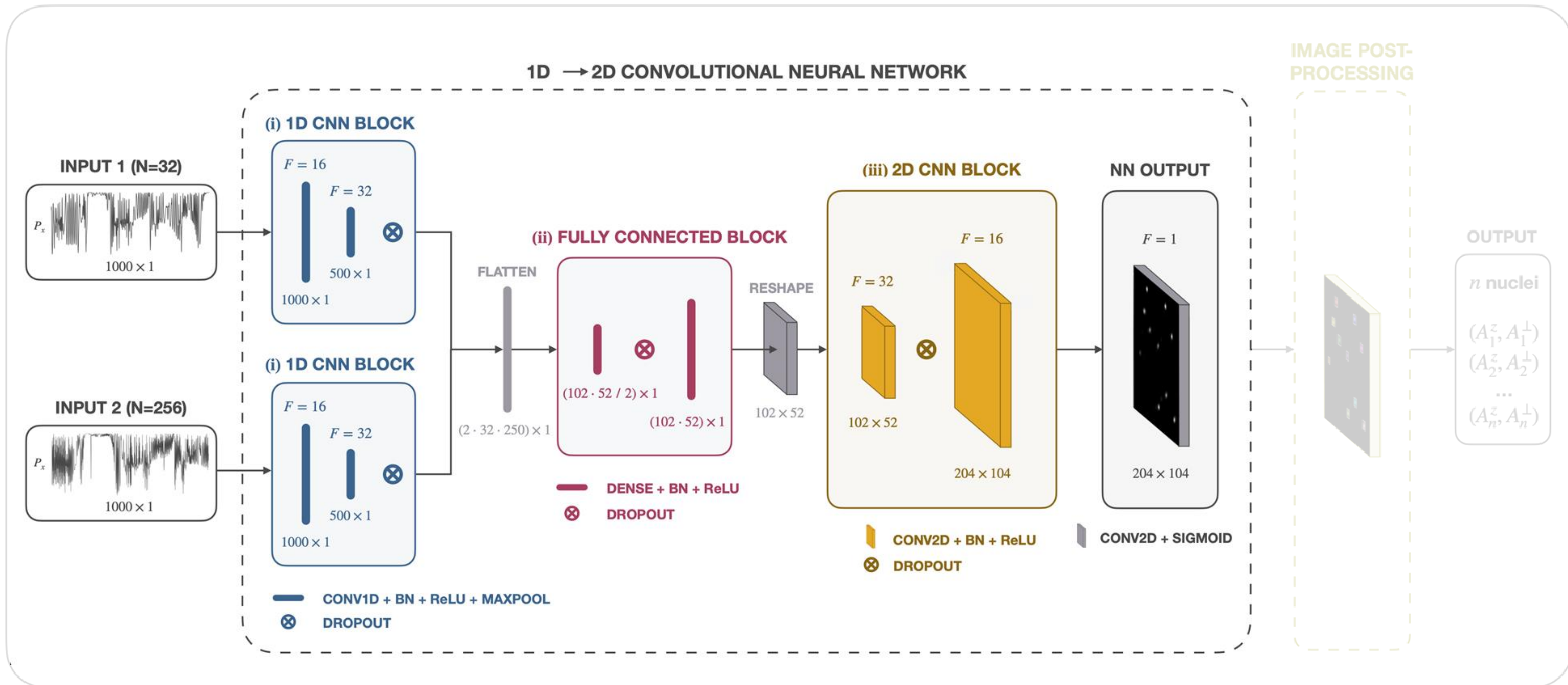
↳ computing each average value of  $P_x$  after simulating  $N_m = 1000$  measurements.



# The SALI model



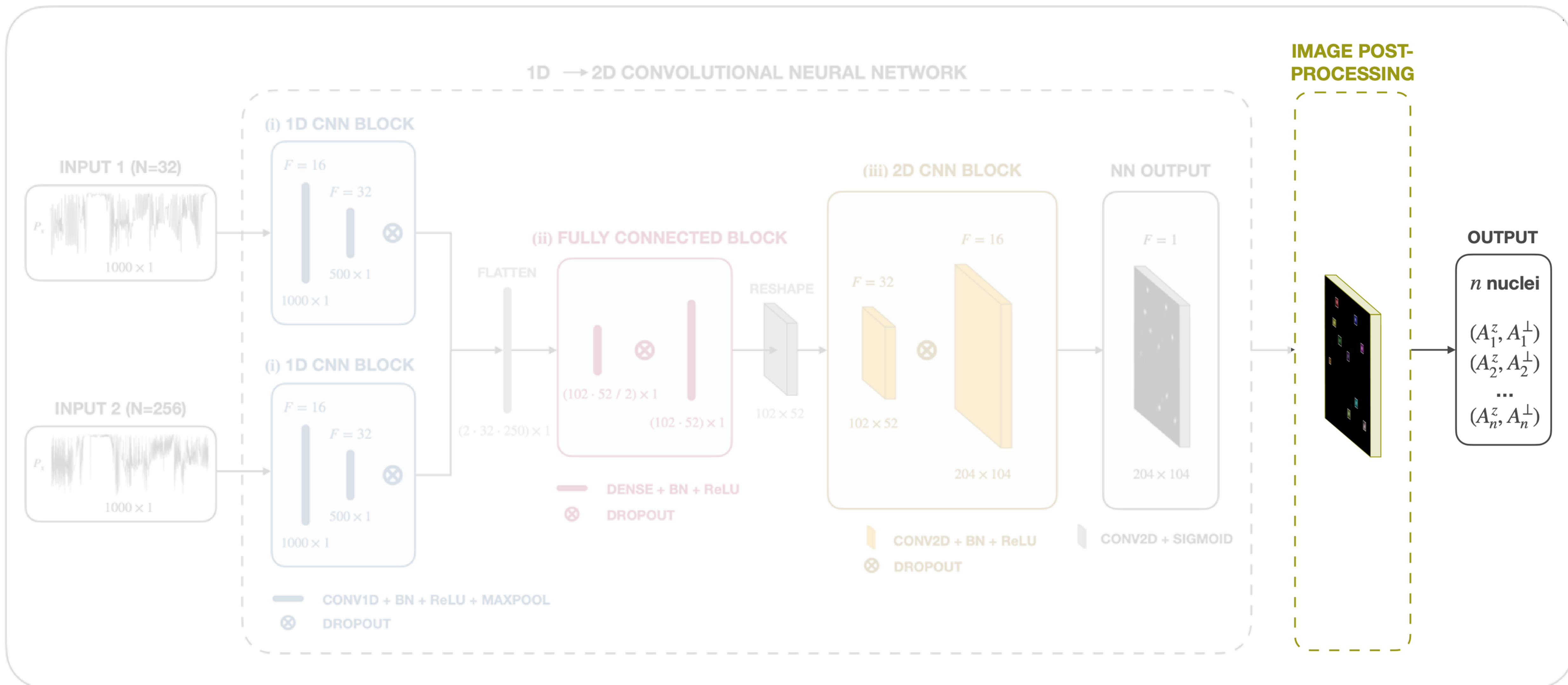
# The SALI model: 1D → 2D CNN



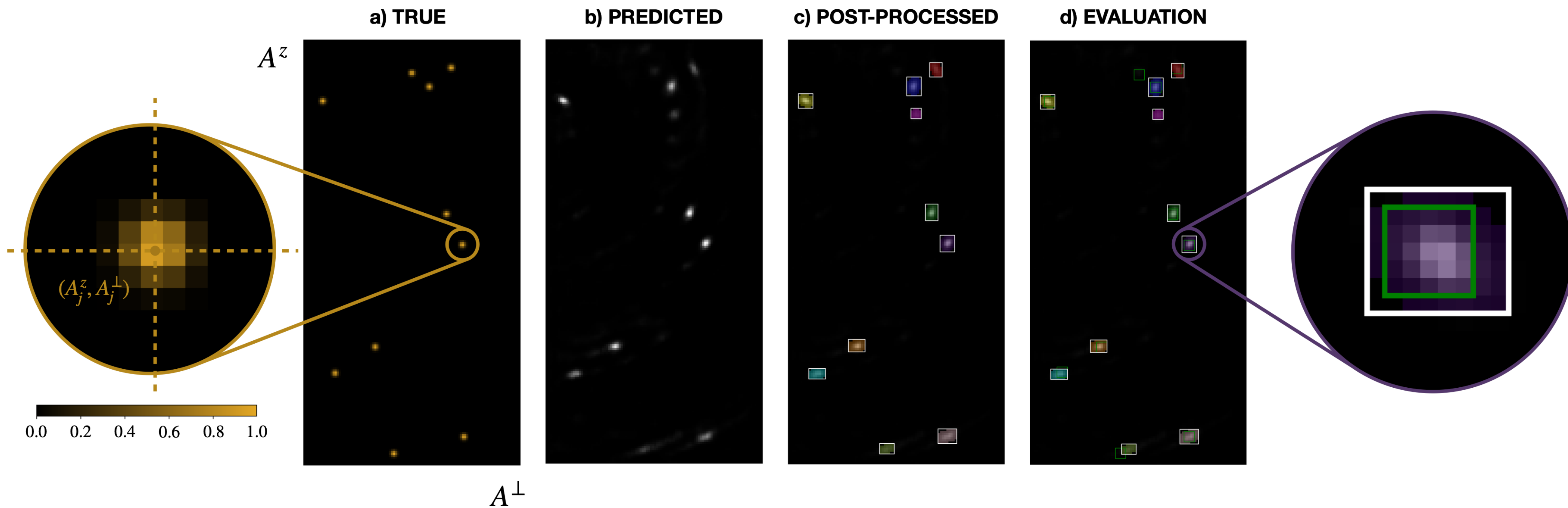
# The SALI model: 1D $\rightarrow$ 2D CNN

- We trained the neural network for both high and low magnetic field scenarios, generating 3.6 M samples for each of the cases.
- Each sample contains a random number of nuclei ranging from 1 to 20.
- Each nucleus is characterized by random values of the coupling constants  $A^Z$  and  $A^\perp$ , falling within the ranges  $A^Z \in [-100, 100]$  kHz and  $A^\perp \in [2, 102]$  kHz.
- This results in a set of coupling constants  $(A_j^Z, A_j^\perp)$  for each sample.
- Nuclei are represented as 'points' in the true output image.

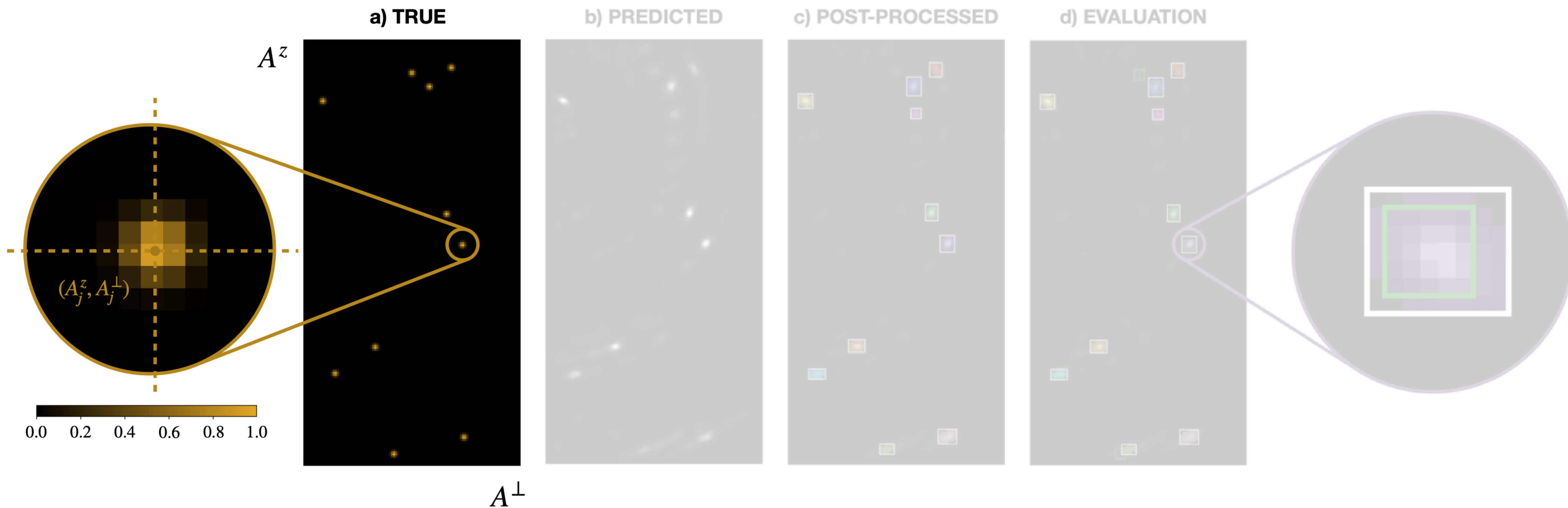
# The SALI model: image post-processing



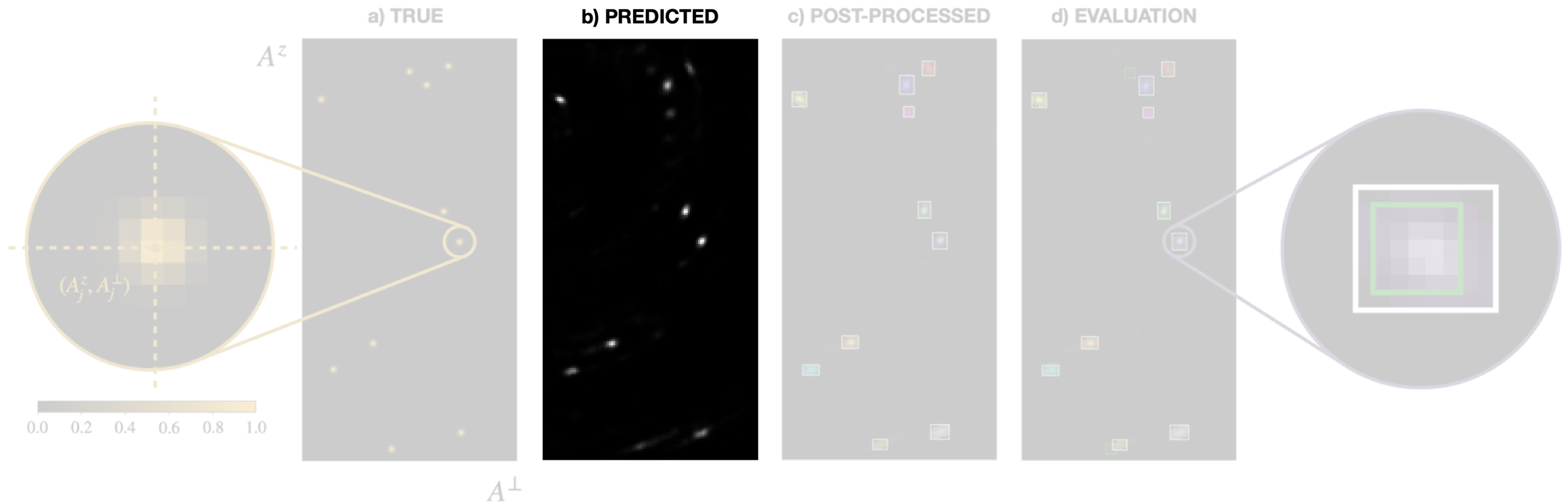
# The SALI model: image post-processing



# The SALI model: image post-processing



# The SALI model: image post-processing

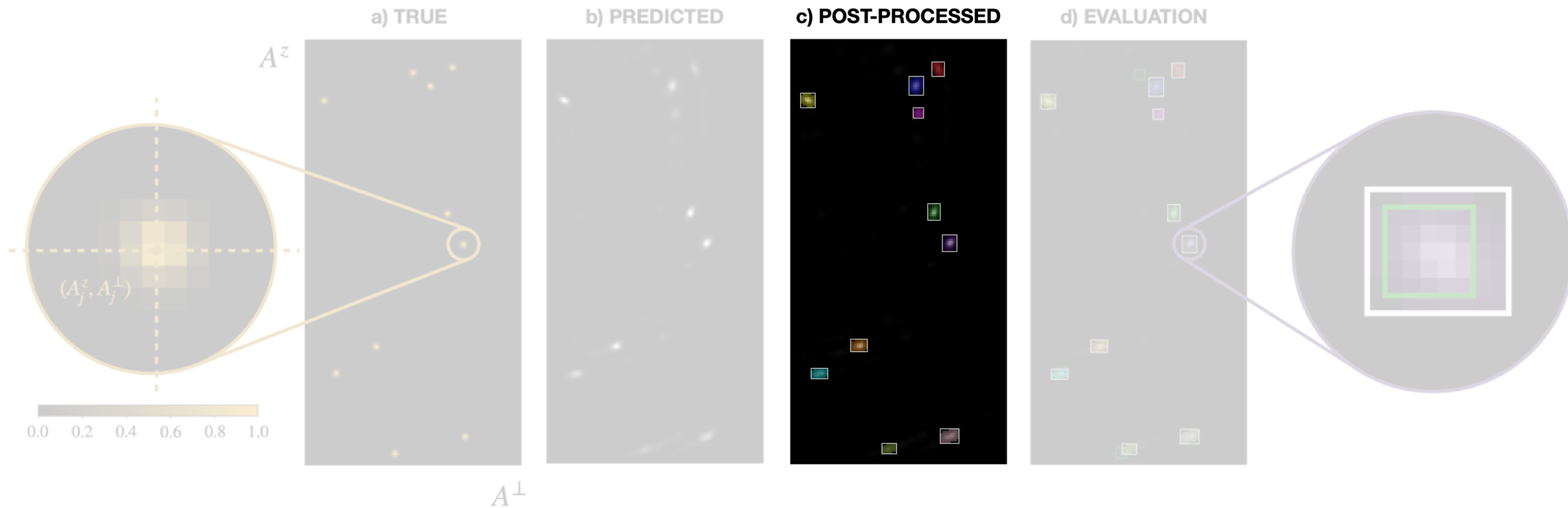


# The SALI model: image post-processing

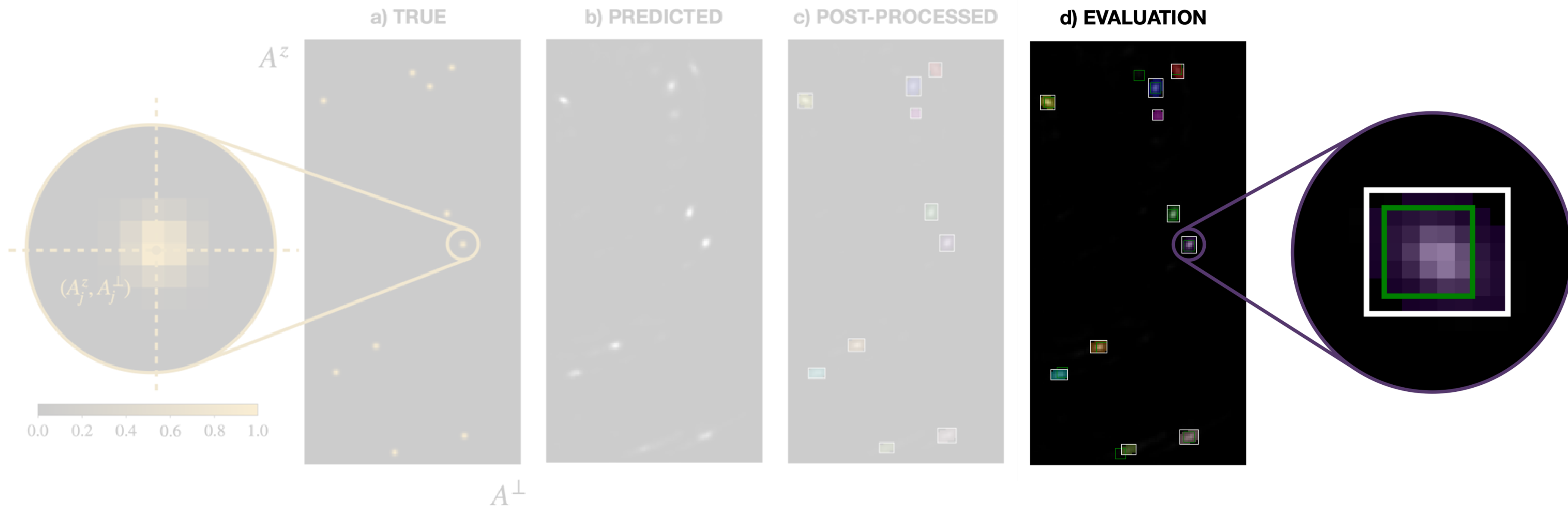
- Erosion and dilation techniques are employed to smooth the image.
- A pixel threshold is applied.
- Adjacent pixels are grouped in clusters using a connectivity routine.
- This results in the prediction of the number of nuclei  $n$  and the corresponding coupling constant pairs  $(A_j^Z, A_j^\perp)$ , which are determined by the centroids of these clusters.



# The SALI model: image post-processing



# The SALI model: image post-processing



# Quantifying the model performance and results

## PRECISION

$$P = \frac{TP}{TP + FP}$$

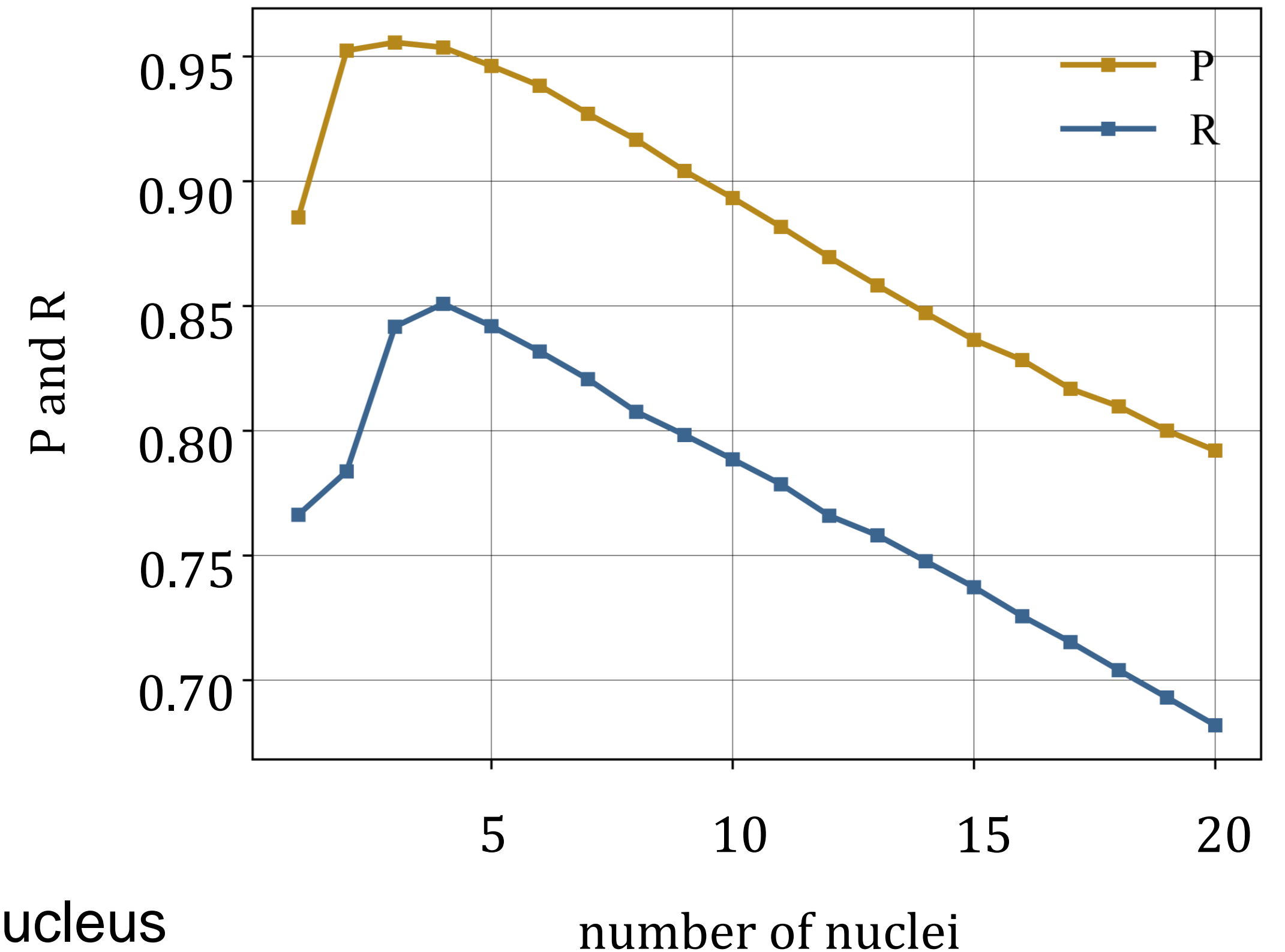
## RECALL

$$R = \frac{TP}{TP + FN}$$

TP: true positive → correctly detected nucleus

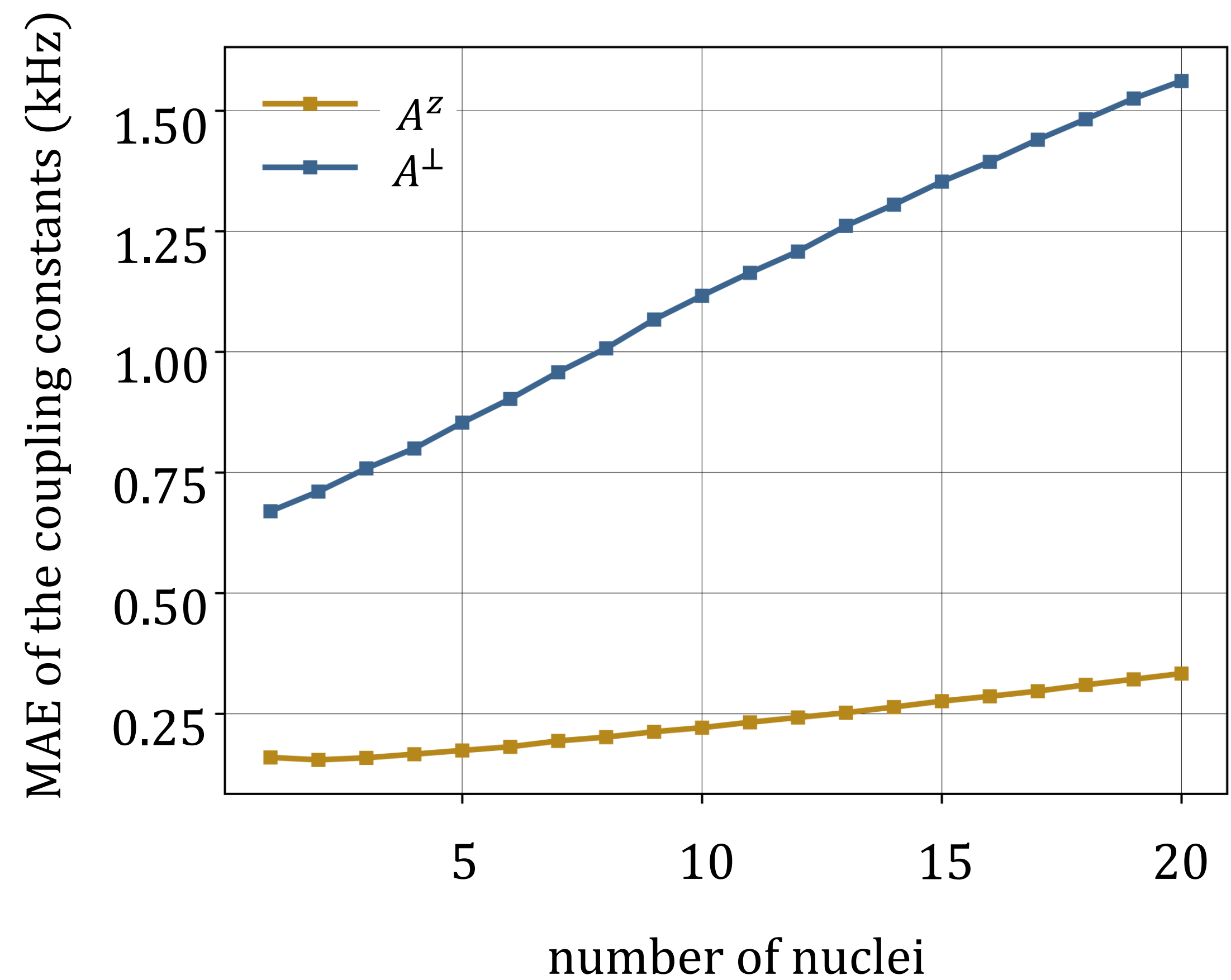
FP : false positive → incorrectly detected non-existent nucleus

FN : false negative → non-detected nucleus



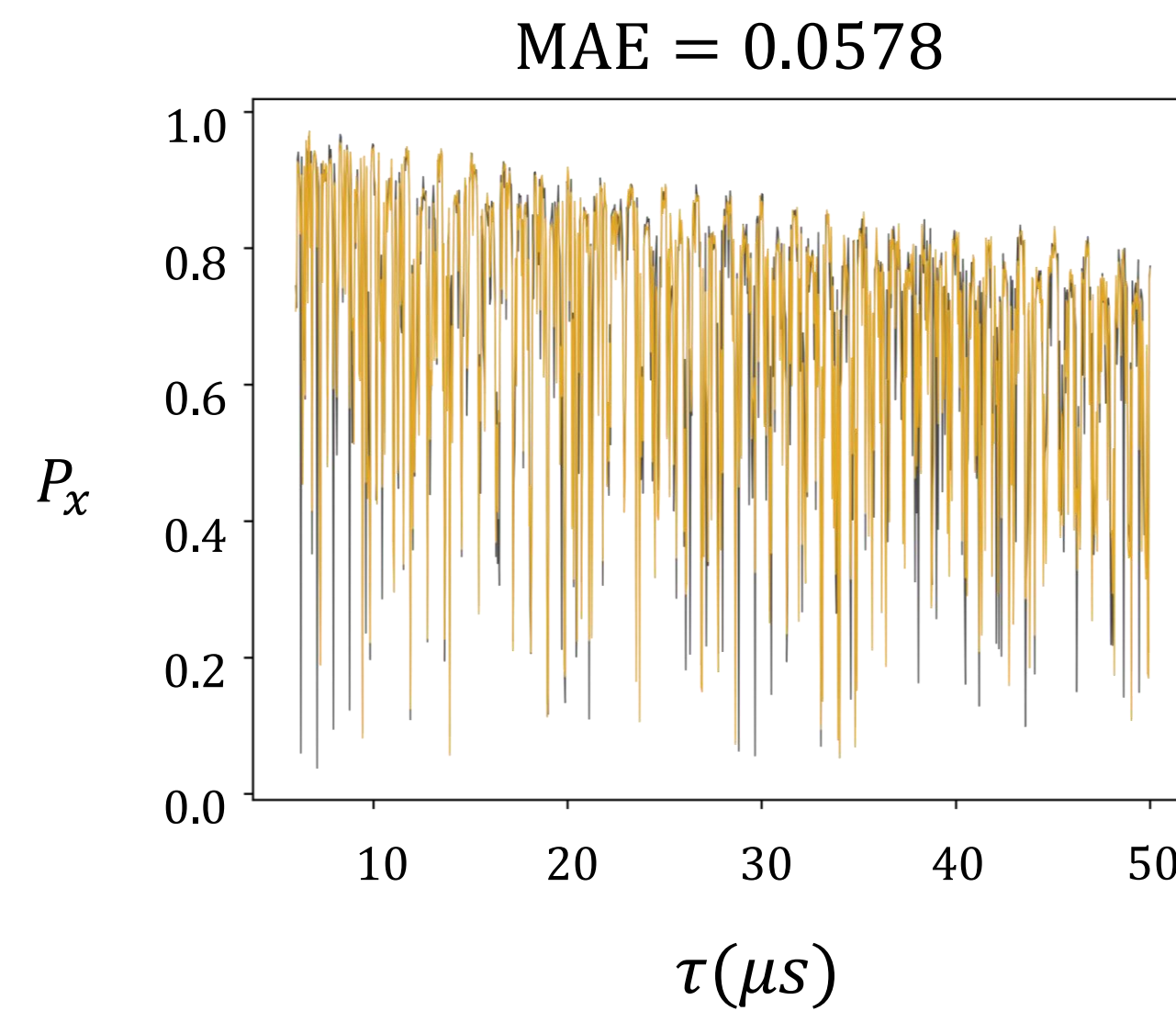
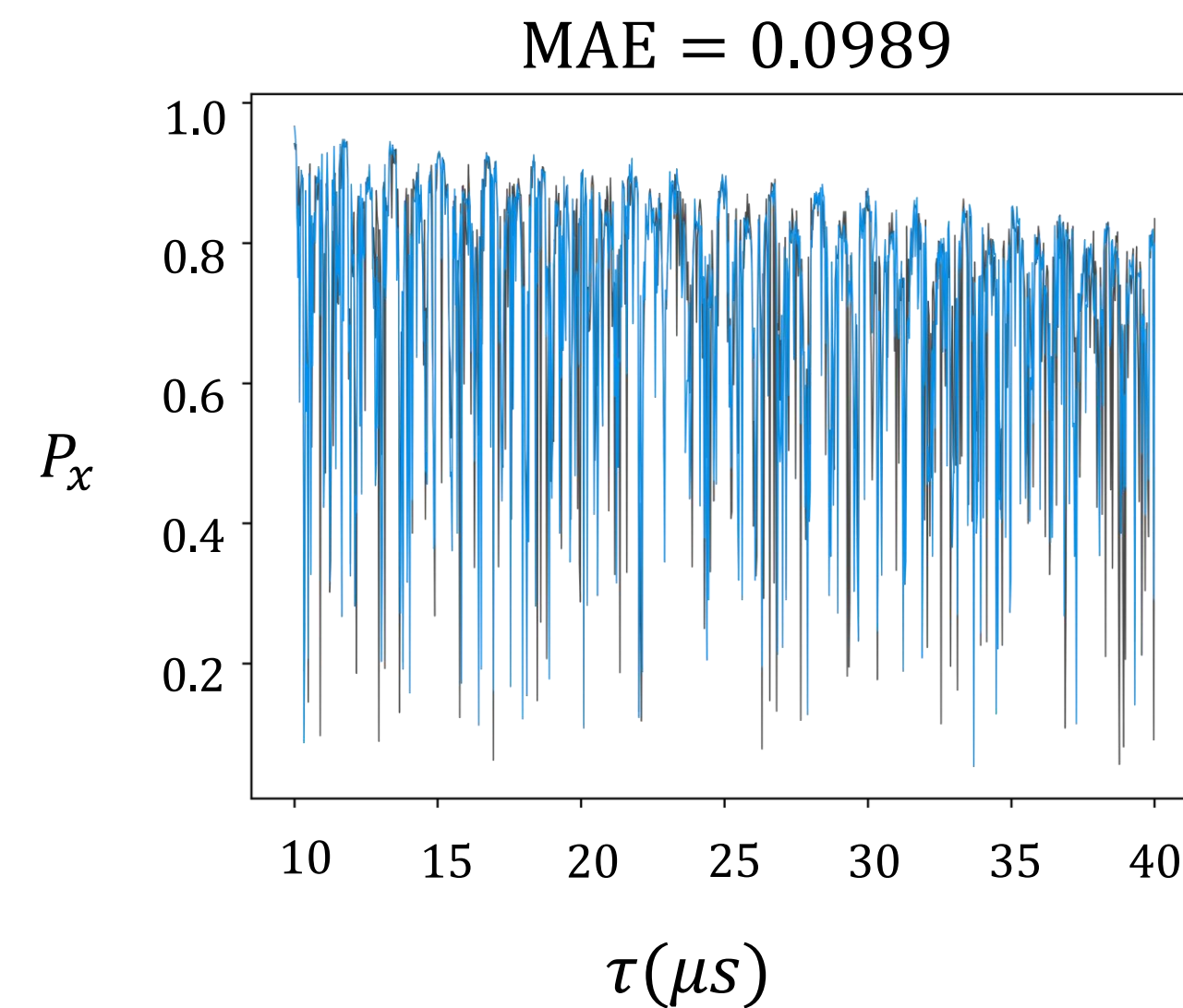
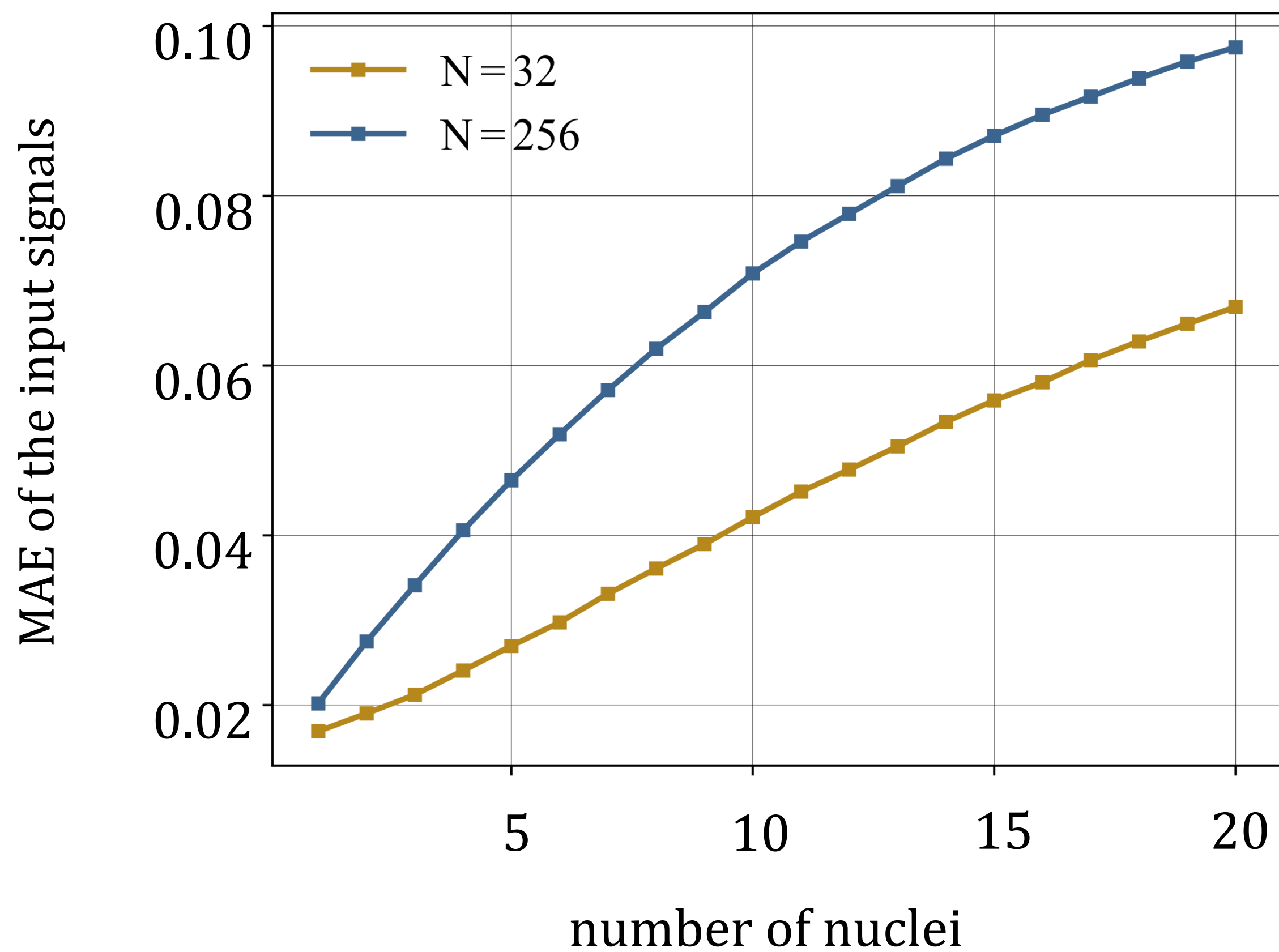
# Quantifying the model performance and results

## MAE of the coupling constants



# Quantifying the model performance and results

## MAE of the input signals



# Reducing experimental time: high magnetic field

- Decrease the number of datapoints by selecting only those that contain relevant information. Preferably, choose points with smaller  $\tau$  values.

# Reducing experimental time: high magnetic field

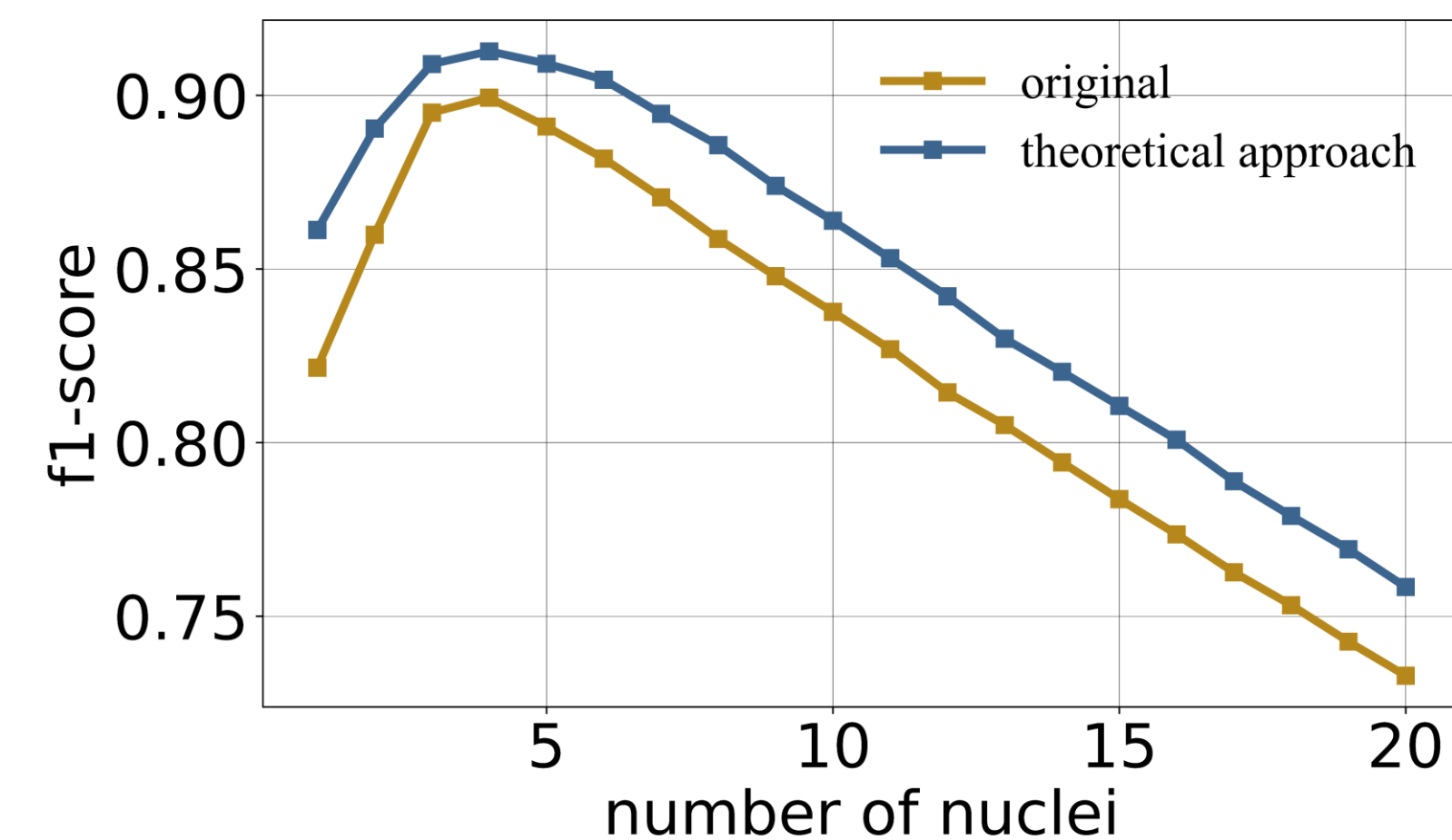
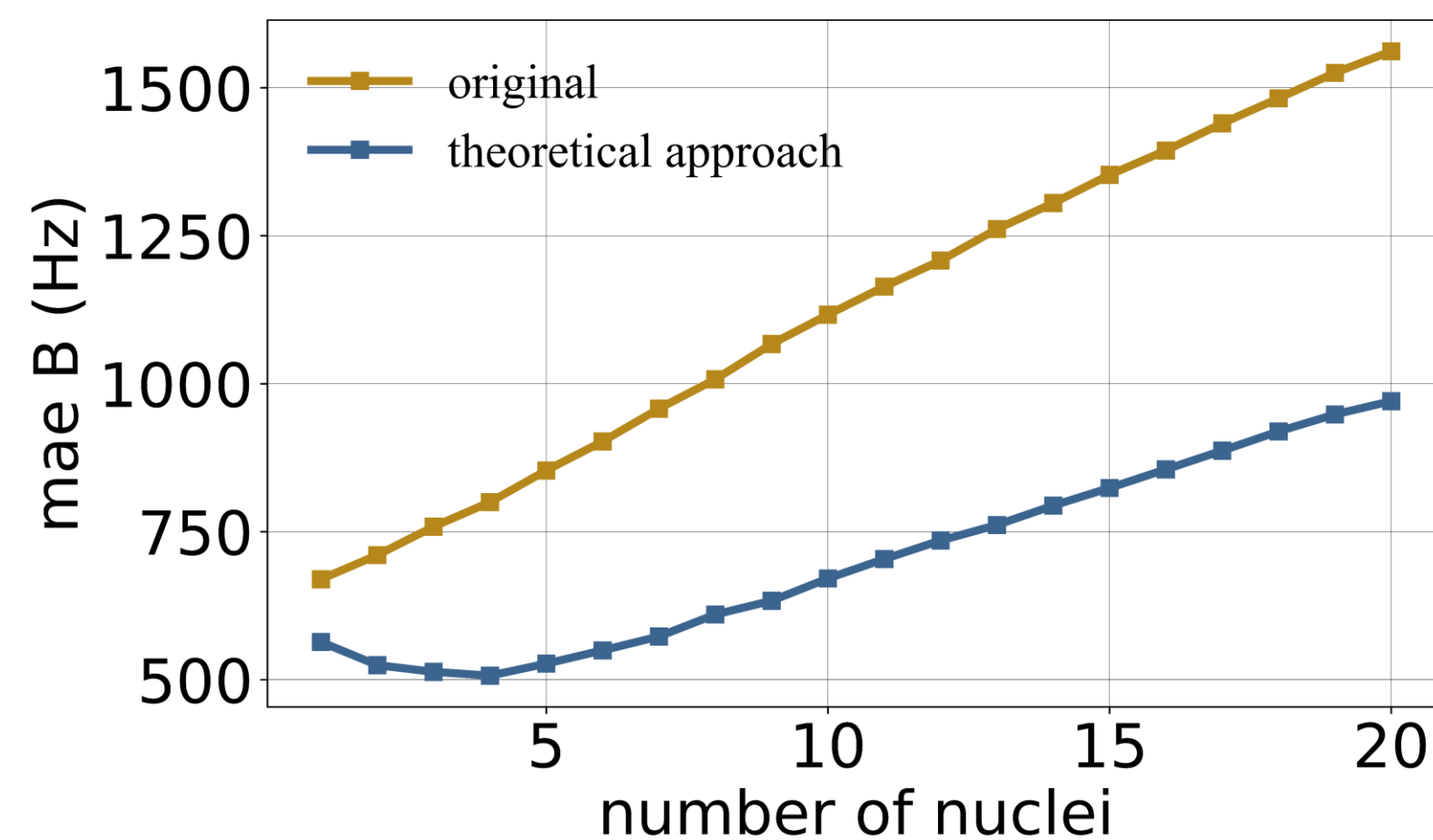
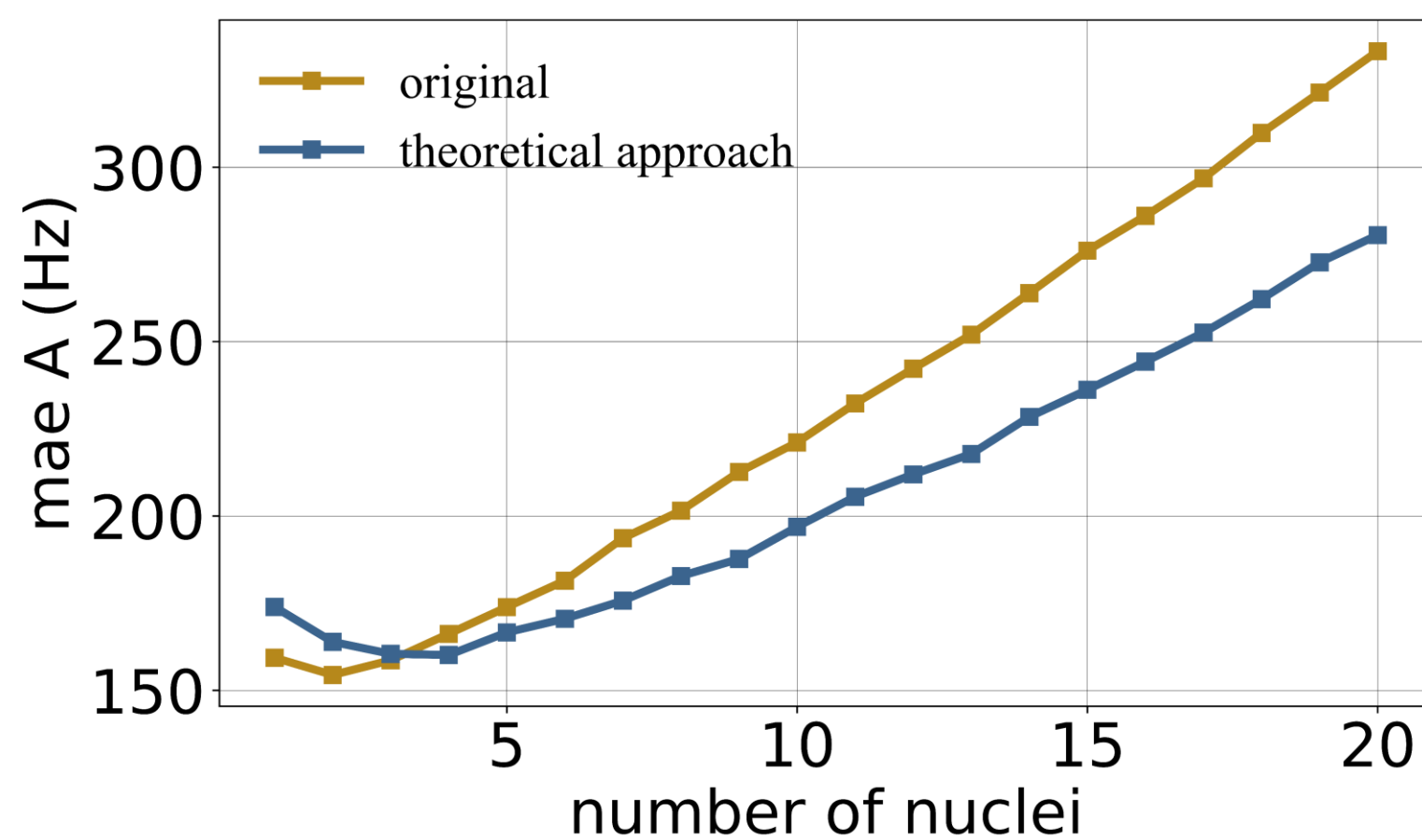
- Decrease the number of datapoints by selecting only those that contain relevant information. Preferably, choose points with smaller  $\tau$  values.
- Strategy:
  1. Scan values of  $\tau$  in the range  $\tau \in [6, 50] \mu\text{s}$  with resolution  $\Delta\tau = 3 \text{ ns}$  and select datapoints based on the prior probability of finding a minimum in the signal:

$$f(\tau) = \frac{(2k - 1)^2}{(2\tau)^2} p\left(\frac{2k - 1}{2\tau} - 2\omega_L\right)$$

2. Select  $N_p$  datapoints by applying a probability threshold.

# Reducing experimental time: high magnetic field

- Selecting  $N_p = 600$  datapoints and simulating  $N_m = 250$  measurements for each results in a total measurement time of **16.80 minutes**, compared to approximately 4 hours required by the original model.
- Despite this reduction in time, the model delivers equal or better performance than the original.





# Outlook and conclusions

- SALI shows potential for use in experimental setups, as it is trained using simulated data that mimics real experimental conditions at both high and low magnetic fields.
- With this training, the model automatically infers the coupling constants between the sensor and nearby  $^{13}\text{C}$  nuclear spins.
- The theoretical approach allows for obtaining the same results in a significantly shorter time, enhancing its practicality for real-world applications.
- Next step: testing the model with actual experimental data. Initially, assess the original model to confirm its functionality. Then, test the model with data derived from the theoretical approach.

**Thank you for your attention!**